THE INFLUENCE OF REAL GAS EFFECTS ON THERMALLY INDUCED LOSSES IN RECIPROCATING PISTON-CYLINDER SYSTEMS

Taleb A.I.[1,*], Barfuss C.[1], Sapin P.[1], White A.J.[2], Willich C.[2], Fabris D.[1,3] and Markides C.N.[1]

[*]Author for correspondence
E-mail: a.taleb@imperial.ac.uk

[1]Clean Energy Processes (CEP) Laboratory,
Deparment of Chemical Engineering,
Imperial College London,
London SW7 2AZ,
United Kingdom

[2]Department of Engineering,
University of Cambridge,
Cambridge CB2 1PZ,
United Kingdom

[3]Department of Mechanical Engineering,
Santa Clara University,
Santa Clara, CA 95053,
USA

ABSTRACT

The efficiency of expanders is of prime importance for various clean energy technologies. Once mechanical losses (e.g. through valves) are minimized, losses due to unsteady heat exchange between the working fluid and the solid walls of the containing device can become the dominant loss mechanism. In this device, gas spring devices are investigated numerically in order to focus explicitly on the thermodynamic losses that arise due to this unsteady heat transfer. The specific aim of this study is to investigate the behaviour of real gases in gas springs and compare this to that of ideal gases in order to attain a better understanding of the impact of real gas effects on the thermally losses in reciprocating piston expanders and compressors. A CFD-model of a gas spring is developed in OpenFOAM. Three different gas models are compared: an ideal gas model with constant thermodynamic and transport properties; an ideal gas model with temperature-dependent properties; and a real gas model using the Peng-Robinson equation of state with temperature and pressure-dependent properties. Results indicate that, for simple, mono- and diatomic gases like helium or nitrogen, there is a negligible difference in the pressure and temperature oscillations over a cycle between the ideal and real gas models. However, when looking at a heavier (organic) molecule such as propane, the ideal gas model tends to overestimate the temperature and pressure compared to the real gas model, especially if no temperature dependency of thermodynamic properties is taken into account. Additionally, the ideal gas model (both alternatives) underestimates the thermally induced loss compared to the real gas model for heavier gases. Real gas effects must be taken into account in order to predict accurately the thermally induced loss when using heavy molecules in such devices.

NOMENCLATURE

Co	[-]	Courant number
c_p	[J/kg·K]	specific heat capacity at constant pressure
c_v	[J/kg·K]	specific heat capacity at constant volume
D	[m]	bore diameter
D_h	[m]	hydraulic diameter at mid-stroke
L_r	[m]	connecting rod length
L_dv	[m]	dead volume height
L_s	[m]	stroke length
r_s	[m]	crank radius
P	[Pa]	pressure
P_0	[Pa]	cycle mean pressure
Pe	[-]	Péclet number
R_m	[J/kg·K]	specific gas constant
Re	[-]	Reynolds number
T	[K]	temperature
T_r	[K]	reduced temperature
v	[m^3/kg]	specific volume
V	[m^3]	volume
V_0	[m^3]	cycle mean volume
V_m	[m^3/mol]	molar volume
Greek characters		
α_0	[m^2/s]	cycle mean thermal diffusivity
γ	[-]	ratio of specific heats
ω	[rad/s]	rotational velocity
ρ	[kg/m^3]	density
ψ	[-]	thermal loss parameter
Abbreviations		
BDC		bottom dead center
CFD		computational fluid dynamics
ORC		organic Rankine cycle
PISO		pressure-implicit split operator
RPM		revolutions per minute
SIMPLE		semi-implicit method for pressure linked equations
TDC		top dead center

INTRODUCTION

Reciprocating machines have potential applications for the efficient conversion of low-grade heat (e.g. solar, geothermal, waste heat). Piston expanders, for instance, are a viable alternative to turbomachines in organic Rankine cycles (ORCs). They provide higher efficiencies at low power outputs and at off-design rotational speeds which may occur due to the intermittent nature of low-grade heat sources. Examples of reciprocating machines for low-grade heat conversion include thermofluidic oscillators [1; 2] and liquid piston Fluidyne engines [3; 4] which rely on liquid pistons to transfer energy from the oscillating pressure and volume of an enclosed working fluid.

In reciprocating machines, irreversible losses occur due to mechanical friction with moving parts, flow losses in valves, and irreversibilities due to heat transfer across a finite temperature difference. Once mechanical losses are minimized, thermally in-

duced losses can begin to dominate and must be taken into account. Performance losses arising due to unsteady heat transfer occur even if the overall process is globally adiabatic (in the mean), since heat exchange between the gas and the cylinder wall across a finite temperature difference is an inherently irreversible process. Heat is transferred from the gas to the wall during compression when the gas temperature is higher than the wall temperature. During expansion, heat is returned back to the gas as its temperature falls below that of the wall. Even if the net fluctuating heat transfer is zero, a finite exergetic penalty is paid. Therefore, it is of primary importance, to quantify and characterize the heat exchange fluctuations between the fluid and the solid.

To understand the basic irreversibility due to the periodic heat transfer without considering inlet and exit flows, a gas spring—in which a fixed mass undergoes sequential compression and expansion within a closed space—is numerically simulated using computational fluid dynamics. Gas springs do not include the complex effects of valve timing and gas exchange of reciprocating-piston devices while they retain the fluctuating heat exchange phenomena between the cylinder walls and gas. Previous work in this area began with Pfriem [5] who described analytically a phase difference between the heat flux and the temperature difference between the wall and the bulk gas. Lee [6] described the oscillating heat flux by developing a model for a complex Nusselt number at low Péclet numbers (or low frequencies). Experiments were conducted by Kornhauser and Smith [7; 8; 9] from which they calculated the thermal loss for a wide range of Péclet numbers and different compression ratios. Additionally, they proposed empirical Nu-Re correlations which accounted for the aforementioned phase difference with imaginary components. The correlation was only developed for low compression ratios and helium as a working fluid. Lekić and Kok [10] simulated Kornhauser and Smith's experiments with CFD simulations and examined local effects of temperature and pressure in the compression space.

Low-grade heat conversion technologies commonly use commonly use more complex organic working fluids. This is especially valid for ORCs and thermofluidic oscillators which rely on refrigerants and hydrocarbons (common examples are pentane, HFC-245fa or HFC-134a) [11; 12]. In previous studies, Lee [6] considered ideal gases while Kornhauser and Smith [7; 8; 9] experimented with light or noble gases such as hydrogen, helium and argon for which the ideal gas law is an accurate approximation. However, in temperature and pressure ranges relevant in this study (200–600 K, 0.5–10 bar) and for organic fluids real gas effects need to be considered. In this study the irreversibility due to heat transfer is quantified accounting for several real gas effects, different equations of state and variable heat capacities.

METHODOLOGY

Problem setup

The geometry of the piston-cylinder arrangement of the gas spring is defined by the following parameters:

bore diameter: $D = 105$ mm
stroke length: $L_\mathrm{s} = 2 \times r_\mathrm{s} = 78$ mm
connecting rod length: $L_\mathrm{r} = 148.5$ mm
dead volume height: $L_\mathrm{dv} = 14$ mm

The geometry was chosen to match an experimental setup which will be used to validate computational work in the future. The Péclet number, Pe, is used as a dimensionless measure for the rotational speed of the gas spring oscillation:

$$Pe = \frac{\omega D_\mathrm{h}^2}{4\alpha_0}\,, \tag{1}$$

where ω is the rotational velocity, $\alpha_0 = k/\rho c_\mathrm{p}$ is the time-averaged thermal diffusivity and $D_\mathrm{h} = 4V_\mathrm{md}/A_\mathrm{md}$ is the hydraulic diameter at mid-stroke.

To quantify the thermal loss of one complete oscillation cycle, Kornhauser and Smith [8] define a loss parameter ψ_K as the ratio of the lost net work to the adiabatic compression work for an ideal gas with the same cyclic mean pressure:

$$\psi_\mathrm{K} = \frac{\oint P\mathrm{d}V}{P_0 V_0 \left(\frac{P_\mathrm{a}}{P_0}\right)^2 \frac{\gamma-1}{\gamma}}\,, \tag{2}$$

where P_0 and V_0 are the cyclic mean pressure and volume respectively, P_a is the pressure amplitude and γ is the ratio of specific heats.

Geometry and mesh

The CFD model was developed in the open source code OpenFOAM (v. 2.1.1). As the system and geometry is axisymmetric (Fig. 1), the gas spring is modelled in two spatial dimensions and temporally over 10 cycles. The geometry consists of a wedge with a width of 0.02 radians and there is only one layer of cells in circumferential direction. The changing volume of

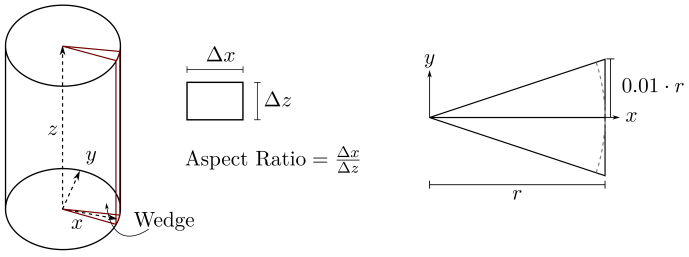

Figure 1: Modelled wedge geometry and defintion of the aspect ratio, left-hand diagram shows the wedge in a perspective view, right-hand diagram shows a top view of the geometry (not to scale).

the compression space is modelled with a dynamic mesh. The moving lower boundary represents the piston. Every node in the mesh compresses vertically relative to the stationary cylinder head (top boundary) and the moving piston head (bottom boundary). Nodes closer to the piston move to a greater extent than

nodes closer to the cylinder head. Thus, the mesh is distorted during compression/expansion as in Fig. 2. The mesh is modelled to have a cell aspect ratio of 1 at mid-stroke so that the distortion at bottom dead center (BDC) and top dead center (TDC) is approximately equal in terms of the ratio of a cell's larger dimension to smaller dimension (if grading is not considered). The size of the cells decreases gradually towards the boundaries to increase the mesh resolution inside the boundary layers near the walls. At midstroke, the smallest cell radial dimension is one fourth of the largest cell radial dimension. The same is valid in axial direction. The mesh resolution used depends on the rotational speed where the total number of cells increases for higher speeds. A convergence study was carried out to investigate the independence of the results from the mesh resolution and the Courant number. For speeds around 100 RPM, for example, the mesh is sufficiently resolved at 90×90 [13].

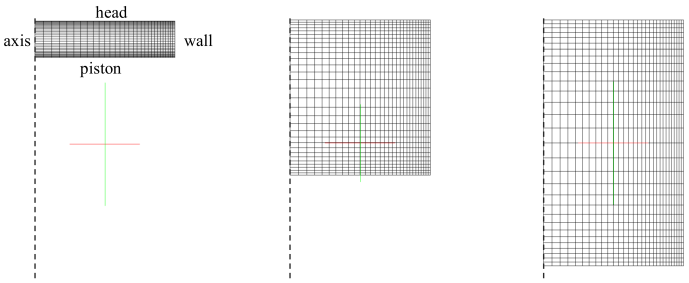

Figure 2: Mesh movement during an expansion stroke of a 30×30 mesh. A grading factor increases resolution near the walls.

The time step is controlled by a user-specified maximum Courant number $Co_{\max}$. For a given cell, the maximum Courant number is defined as:

$$Co_{\max} = \frac{|u|\Delta t}{\Delta x}\,, \tag{3}$$

where $|u|$ is the magnitude of the velocity through a cell, Δx is the cell size in the direction of the velocity and Δt is the time step. The time step is chosen such that $Co_{\max}$ is never exceeded. Due to the dynamic mesh, the time step not only adapts to the flow velocity but also to the change in cell size. For speeds around 100 RPM, the maximum Courant number chosen is $Co_{\max} = 0.1$.

The compressible solver uses a modified version of *coldEngineFOAM*, provided by OpenFOAM for piston engines without combustion. It is based on the PIMPLE algorithm which is a combination of the SIMPLE (semi-implicit method for pressure linked equations) and PISO (pressure-implicit split operator).

Turbulence model

The simulations have shown that during the upstroke and the downstroke the velocity profile is primarily axial and uniform in radial direction. There is only a significant gradient in axial direction, which is expected from the piston movement. Turbulence is generated in regions of high perpendicular velocity gradients to the main flow direction. This requires a sufficiently high convective force to overcome the damping effect of the viscosity. This can occur in the boundary layer during the stroke or in a roll up vortex which is produced at the contact point of the piston and cylinder wall. Considering the maximum piston velocity of $u_{\max} = 4.084$ m/s at the highest considered speed of 1000 RPM, the Reynolds number is $Re = 27170$ in the boundary layer. Because of the absence of perpendicular gradients, the uniform core flow is considered to be laminar and has no effect on turbulence generation in the boundary layer. Thus the boundary can be compared to an impulsive boundary layer on a rotary disk. Chin and Litt [14] state for experiments on transition of a boundary layer on smooth rotary disks a critical Reynolds number of 170000. Since the operating conditions modelled are at a Reynolds number which is one order of magnitude lower, the boundary layer is not considered turbulent or transitional. It should be noted that the unsteady simulation does capture the large scale vortex roll-up motion. Lekić and Kok [10] simulated both laminar and turbulent cases and found that turbulence has a negligible impact on the governing physical phenomena in their simulations.

Real gas effects

In this study, both real and ideal gas equations of state are compared. For real gases, the ideal gas equation of state is replaced by the Peng-Robinson equation of state [15]:

$$P = \frac{RT}{V_{\mathrm{m}} - b} - \frac{a\alpha}{V_{\mathrm{m}}\left(V_{\mathrm{m}} + b\right) + b\left(V_{\mathrm{m}} - b\right)}\,, \tag{4}$$

where V_{m} is the molar volume; and a, b and α are the attraction parameter, van der Waals covolume and scaling factor respectively, defined in the following:

$$a = 0.45724\frac{R^2 T_{\mathrm{c}}^2}{P_{\mathrm{c}}} \quad b = 0.07780\frac{RT_{\mathrm{c}}}{P_{\mathrm{c}}}\,. \tag{5}$$

R is the universal gas constant, T_{c} and P_{c} are the critical temperature and pressure.

$$\alpha = \left(1 + \kappa\left(1 - T_{\mathrm{r}}^{1/2}\right)\right)^2\,, \tag{6}$$

where T_{r} is the reduced temperature, $\kappa = 0.37464 + 1.54226\omega_{\mathrm{z}} - 0.26992\omega_{\mathrm{z}}^2$ and ω_{z} is the acentric factor. Additionally, the temperature dependent mass-specific heat capacity $c_p^0(T)$, enthalpy $h^0(T)$ and entropy $s^0(T)$ for ideal gases are calculated with temperature dependent polynomials often referred to as JANAF or NASA heat capacity polynomials [16]. For brevity, only the heat capacity is shown here:

$$c_{\mathrm{p}}^0(T) = R_{\mathrm{m}}\left(a_1 T^{-2} + a_2 T^{-1} + a_3 + \right. \\ \left. + a_4 T + a_5 T^2 + a_6 T^3 + a_7 T^4\right)\,, \tag{7}$$

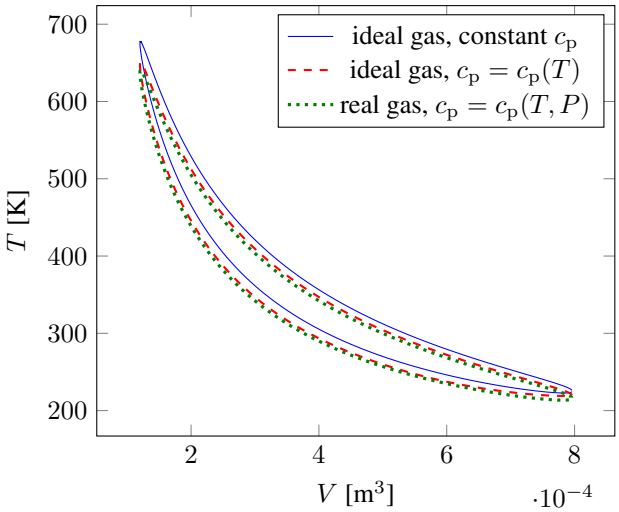

Figure 3: T-V diagram for helium at 500 RPM, $Pe \approx 300$.

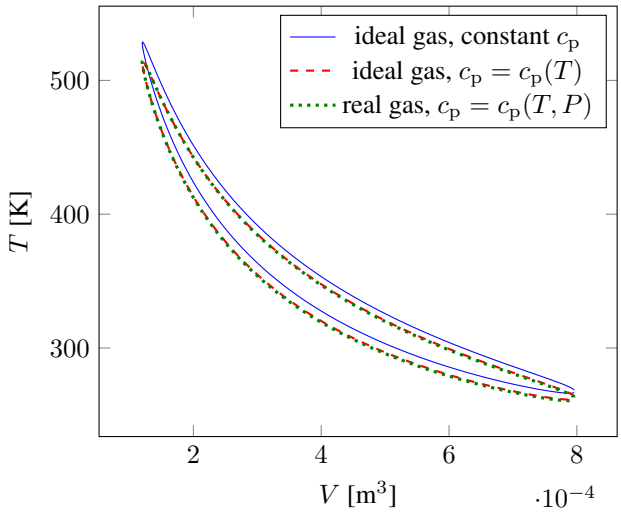

Figure 4: T-V diagram for nitrogen at 70 RPM, $Pe \approx 300$.

where $R_m = R/M$ is the specific gas constant. With

$$\left(\frac{\partial c_p}{\partial v}\right)_T = -T\left(\frac{\partial^2 v}{\partial T^2}\right)_P , \tag{8}$$

a correction for the pressure dependency of c_p can be calculated [17]:

$$c_p(T,P) = c_p^0(T) - T\int_0^P \left(\frac{\partial^2 v}{\partial T^2}\right)_P \mathrm{d}P , \tag{9}$$

where v is the specific volume.

Initial and boundary conditions

Initial conditions of the pressure and temperature are set at BDC (crank angle $\phi = -180\ °$). For all cases, the initial pressure and temperature are set at 1 bar and 330 K. The wall temperatures are uniform and constant at 350 K. Adair et al. [18] observed in their experiments that the cylinder wall temperatures in reciprocating compressors oscillate by less than 1 K. The same temperature was selected for all wall boundaries (cylinder head, piston head and cylinder wall). The CFD simulations of Lekić and Kok [10] made the same assumption of constant and uniform wall temperature.

RESULTS

Influence of real gas effects on temperature and pressure

Three gases were considered in this study: helium, nitrogen and propane. Nitrogen as well as helium are expected to behave as ideal gases. Propane, however, is expected to deviate from the ideal gas behaviour due to the increased complexity of the molecule. To compare the three gases, a similar Peclét number of $Pe \approx 300$ was adopted which arose for 500 RPM with

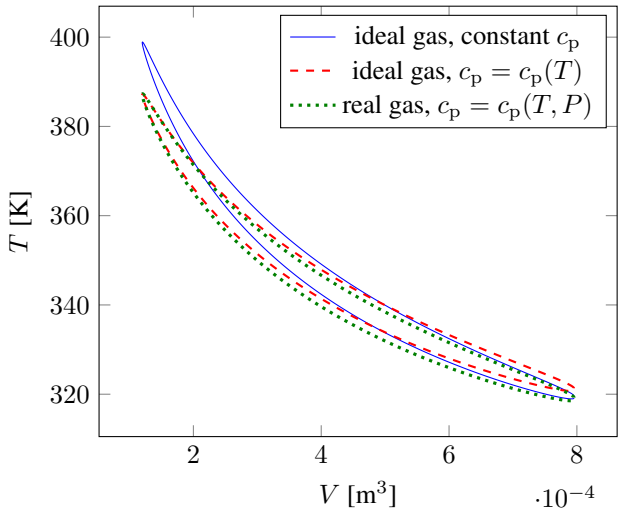

Figure 5: T-V diagram for propane at 20 RPM, $Pe \approx 300$.

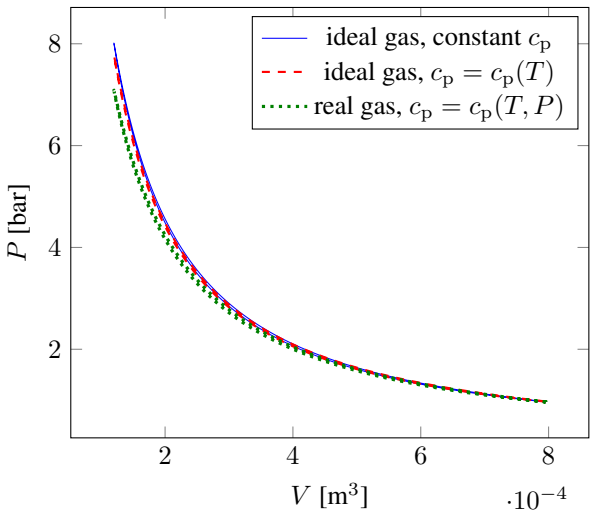

Figure 6: P-V diagram for propane at 20 RPM, $Pe \approx 300$.

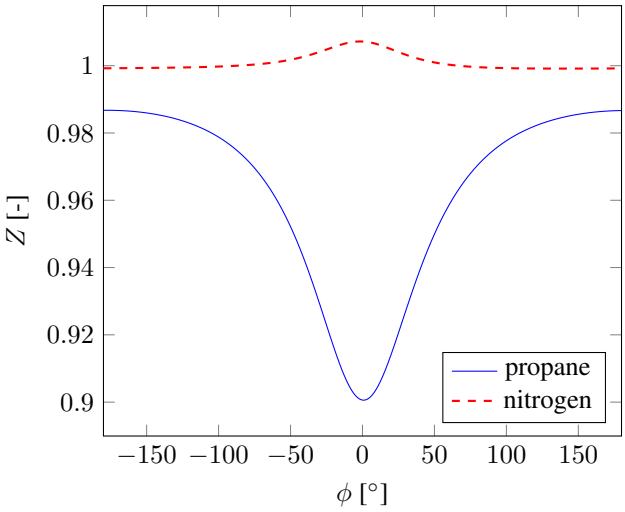

Figure 7: Compressibility Z during one cycle for nitrogen and propane

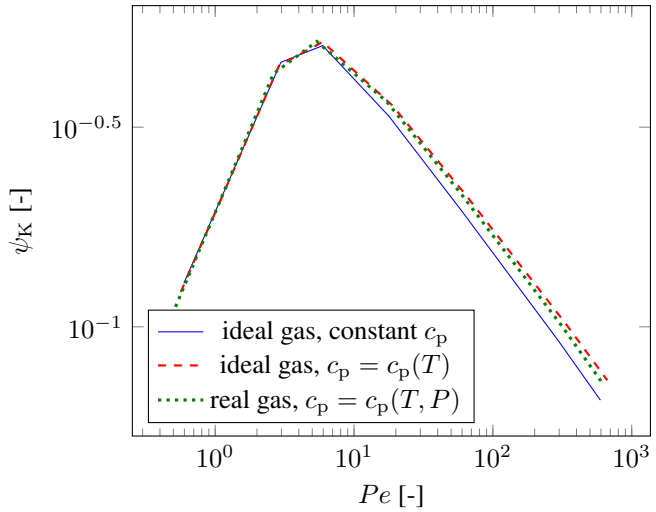

Figure 8: Loss ψ_K for helium.

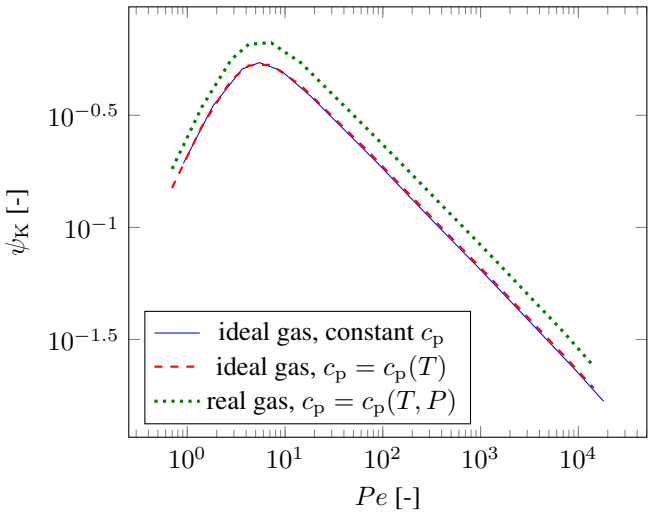

Figure 9: Loss ψ_K for propane.

helium, 70 RPM with nitrogen and 20 RPM with propane. Figures 3–5 show T-V curves for the three substances when modelled as ideal gases with constant (solid blue) and temperature dependent thermodynamic/transport properties (dashed red) and as real gases with pressure and temperature dependent properties (dotted green). As expected, nitrogen and helium behave similarly regardless of the model, although, when assuming constant thermophysical properties the temperatures are slightly overestimated compared to the real gas model. Propane, on the other hand, shows deviations. In Fig. 5, one can see that the constant property ideal gas model (solid blue) overestimates temperatures at TDC by about 3% (high pressure) compared to the real gas model, but at BDC (low pressure) the agreement in temperature is good. The ideal gas model with temperature dependent properties (dashed red) shows good agreement in temperatures at TDC but at low temperatures it shows slight deviation. Figure 6, shows a P-V plot for propane. One can see here that in this case both ideal gas models deviate from the real gas model. Because both ideal gas models do not have a correction for the pressure dependency of the gas properties, they both overestimate the pressure by as much as 14% at TDC (at high pressures) compared to the real gas model. The discrepancy between ideal and real gases can be understood with the compressibility factor $Z = Pv/RT$ plotted in Fig. 7. For ideal gases, $Z = 1$. A value different from unity provides a measure for the magnitude of the real gas effects. These tend to increase when one is close to the critical point or saturation, so for the cases considered, at low temperatures and high pressures. Figure 7 shows that Z is almost always equal to 1 at all crank angles for nitrogen. When propane is used, Z moves away from 1 at TDC. The largest differences between the ideal and real gas models are observed at this position.

Thermally induced losses

Figures 8 and 9 show the loss parameter ψ_K for helium and propane for varying Péclet numbers. The general trend which has been reported in previous work [6; 7; 8; 10; 19] is also observed here: at low and high Peclét numbers the loss is low and it reaches a maximum at an intermediate value which is around $Pe \approx 10$. At low Peclét numbers, the oscillation frequency is small such that any work done by the gas will be exchanged in the form of heat with the solid walls. The gas temperature remains constant and equal to the wall temperature. The system undergoes isothermal compression. On the other hand, at high Peclét numbers the oscillation frequency is high. The variation between compression and expansion occurs too quickly for significant heat transfer to occur. The system experiences adiabatic compression and expansion. Therefore, at intermediate Peclét numbers, the work will result from the interplay between both the internal energy of the gas and the heat transfer to the solid leading to a net loss of work during the cycle.

At low Pe, all three models calculate similar loss values for helium shown in Fig. 8. When moving to $Pe > 10$, one can observe that only the constant property model underestimates the loss compared to the other two alternatives. As for propane (Fig. 9), both ideal gas models underestimate the thermal loss compared to the real gas models. This is for the whole Pe number range. Interestingly, both of the ideal gas models calculate very similar loss values. Real gas effects increase the thermally induced losses significantly, which is not captured with the ideal gas models.

CONCLUSION

A two dimensional CFD model of a gas spring wedge has been developed to simulate the compression/expansion processes and thermally induced losses in gas springs. The model also takes real gas effects into account by calculating pressure and temperature dependent thermodynamic and transport properties and by using the Peng-Robinson equation of state. Due to the low velocity of the flow and piston, the Reynolds number is well below the critical Reynolds numbers for turbulence in the boundary layer, and a laminar model is used. The wall temperatures at the boundaries of the model are uniform and constant.

Three different gas models were compared: (1) an ideal gas model with constant thermodynamic and transport properties, (2) an ideal gas model with temperature dependent properties and (3) a real gas model using the Peng-Robinson equation of state with pressure and temperature dependent properties. When comparing helium and nitrogen at $Pe \approx 300$, all three models show similar variation in pressure and temperature over the cycle. For, propane the ideal gas models deviate from real gas models especially at high pressures occurring at TDC. When comparing to the results of the real gas model, the ideal gas models overestimate the pressures and to a lesser extent the temperatures in these conditions. The compressibility factor Z is almost always 1, but for propane at TDC Z falls down to 0.9. This explains the discrepancies between the ideal and real gas models of propane. Thermally induced losses were compared for the gases at different Péclet numbers. Differences between the models were observed even for helium: the constant property ideal gas model calculates a smaller loss than the other alternatives. For propane, both ideal gas models underestimate the thermal loss compared to the real gas models. This occurs for the whole Péclet number range indicating that real gas effects can increase the thermally induced losses in gas springs.

REFERENCES

[1] Markides C.N., and Smith T.C.B., A dynamic model for the efficiency optimization of an oscillatory low grade heat engine, *Energy*, vol. 36, (2011), pp. 6967–6980

[2] Solanki R., Mathie R., Galindo A., and Markides C.N., Modelling of a two-phase thermofluidic oscillator for low-grade heat utilisation: Accounting for irreversible thermal losses, *Applied Energy*, vol. 106, (2013), pp. 337–354

[3] Stammers C.W., The operation of the Fluidyne heat engine at low differential temperatures, *Journal of Sound and Vibration*, vol. 63, (1979), pp. 507–516

[4] West C.D., Dynamic analysis of the Fluidyne, *Proceedings of the 18th Intersociety Energy, Conversion Engineering Conference*, 1983, pp. 779–784

[5] Pfriem H., Periodic heat transfer at small pressure fluctuations, Tech. rep., National Advisory Committee for Aeronautics, 1943

[6] Lee K.P., A simplistic model of cyclic heat transfer phenomena in closed spaces, *Proceedings of the 18th Intersociety Energy Conversion Engineering Conference*, 1983, pp. 720–723

[7] Kornhauser A.A., and Smith J.L., Application of a complex nusselt number to heat transfer during compression and expansion, *Fluid Flow and Heat Transfer in Reciprocating Machinery*, (1987), pp. 89–96

[8] Kornhauser A.A., and Smith J.L., The effects of heat transfer on gas spring performance, *Journal of Energy Resources Technology*, vol. 115, (1993), pp. 70–75

[9] Kornhauser A.A., and Smith J.L., Application of a complex nusselt number to heat transfer during compression and expansion, *Transactions of the American Society of Mechanical Engineers, Journal of Heat Transfer*, vol. 116, (1994), pp. 536–542

[10] Lekić U., and Kok J., Heat transfer and fluid flows in gas springs, *Open Thermodynamics Journal*, vol. 4, (2010), pp. 13–26

[11] Chen H., Goswami Y.G., and Stefanakos E.K., A review of thermodynamic cycles and working fluids for the conversion of low-grade heat, *Renewable and Sustainable Energy Reviews*, vol. 14, (2010), pp. 3059–3067

[12] Quoilin S., Broek M.V.D., Declaye S., Dewallef P., and Lemort V., Techno-economic survey of organic rankine cycle (orc) systms, *Renewable and Sustainable Energy Reviews*, vol. 22, (2013), pp. 168–186

[13] Barfuß C., *Numerical Simulation of Heat Transfer Effects during Compression and Expansion in Gas Springs*, Master's thesis, Technicshe Universität München, 2016, in preparation

[14] Chin D.T., and Litt M., An electrochemical study of flow instability on a rotating disk, *Journal of Fluid Mechanics*, vol. 54, (1972), pp. 613–625

[15] Peng D.Y., and Robinson D.B., A new two-constant equation of state, *Industrial & Engineering Chemistry Fundamentals*, vol. 15, (1976), pp. 59–64

[16] Burcat A., and Ruscic B., Third millennium ideal gas and condensed phase thermochemical database for combustion with updates from active thermochemical tables, Tech. Rep. ANL-05/20, Argonne National Laboratory, 2005

[17] Çengel Y.A., and Boles M., *Thermodynamics: An Engineering Approach*, McGraw–Hill, 2005

[18] Adair R.P., Qvale E.B., and Pearson J.T., Instantaneous heat transfer to the cylinder wall in reciprocating compressors, *International Compressor Engineering Conference*, 1972

[19] Mathie R., Markides C.N., and White A.J., A framework for the analysis of thermal losses in reciprocating compressors and expanders, *Heat Transfer Engineering*, vol. 35, (2014), pp. 1435–1449